Innovative metallic solutions for alpine ski bases

Francesco Ripamonti, Valentina Furlan, Ali G. Demir, Barbara Previtali, Michele Derai, Federico Cheli, and Paolo M. Ossi

Citation: Journal of Vacuum Science & Technology B, Nanotechnology and Microelectronics: Materials, Processing, Measurement, and Phenomena **36**, 01A108 (2018);

View online: https://doi.org/10.1116/1.5002542

View Table of Contents: http://avs.scitation.org/toc/jvb/36/1

Published by the American Vacuum Society

Innovative metallic solutions for alpine ski bases

Francesco Ripamonti,[a] Valentina Furlan, Ali G. Demir, Barbara Previtali, Michele Derai, and Federico Cheli
Department of Mechanical Engineering, Politecnico di Milano, Via La Masa 1, 20156 Milan, Italy

Paolo M. Ossi
Department of Energy, Politecnico di Milano, Via Ponzio 34-3, 20133 Milan, Italy

(Received 30 August 2017; accepted 9 January 2018; published 18 January 2018)

Ski manufacturers are interested in improving ski performance in terms of rapid sliding, excellent trajectory control, and reduced maintenance. A possible approach to achieve this goal is based on substitution of the base material, moving from the standard ultra-high-molecular-weight polyethylene to metallic solutions. Despite their elevated mechanical properties, however, metallic materials exhibit a poor sliding behavior, at least in their original manufacture condition. Although the interaction between the ski base and snow is still an open field, the authors investigated the relationship between ice friction and material hydrophobicity. The wettability behavior of surfaces can be managed by surface patterning techniques, among which laser surface texturing (LST) is a promising method, permitting surface feature modification from the micrometer- to millimeter-scale, and attractive for industrial applications. Herein, the tribological properties of two metallic materials are investigated and a process to reduce the sliding friction against snow is proposed. The LST is used to realize dimple patterning on the metallic surfaces, where the laser parameters are used to control the dimple geometry and surface wettability using untreated substrates as a reference condition. Finally, characterization using a prototype snow tribometer was performed to determine the friction coefficient and sliding performance of the laser-treated metallic surfaces. *Published by the AVS.* https://doi.org/10.1116/1.5002542

I. INTRODUCTION

Among technology products, sports equipment is subjected to the most relevant innovations. For example, the skis used for alpine skiing must demonstrate the capability of easy and controlled direction changes, vibration damping, considerable bending stiffness, high torsion rigidity, low friction against snow, and, if possible, low weight. The latest relevant innovation in the ski-manufacturing field, which dates back to the 1990s, concerned the edge profile design, which allows the ski edge to carve a precise trajectory, once the ski, being inclined at a given rake angle on the snow, is flexed by the skier. Since that time, no innovation regarding the use of different materials of surface structures has been introduced in the manufacturing of conventional skis. Nowadays, ski producers are interested in new solutions to improve ski performance and maintenance. Focusing on the ski base, our starting point was the concept of a new ski structure breakthrough based on an innovative metallic base. Metallic materials such as stainless steel or aluminum have better mechanical properties than ultra-high-molecular-weight polyethylene (UHMWPE), which is the only material used presently for ski base manufacturing. The use of metallic materials would permit a reduction in the number of layers that constitute the ski structure, as well as rendering the addition of metal ski edges unnecessary. In fact, a metallic ski base, once suitably shaped and sharpened on the edges, would comprise a substitute for the usual low-carbon-steel edges presently used. On the other hand, metallic materials show inferior performances in terms of the friction coefficient in contact with snow and ice compared to properly waxed UHMWPE. For this reason, to exploit the advantages of metallic materials, the friction behavior of metallic materials on snow and ice should be improved.

Regarding ice friction, Kietzig *et al*. have described the different states involved, where the water passes from solid to liquid throughout the interaction. Moving from an ice– solid interaction (without lubrication) to a condition with a consistent layer of liquid, it is possible to identify four main states:[1]

(1) dry friction,
(2) boundary lubrication,
(3) mixed friction, and
(4) hydrodynamic lubrication,

where reduced friction coefficient values are achieved by boundary lubrication and the mixed friction state.[1] The parameters of relevance when considering the friction occurring in an ice/solid system have been identified as temperature,[1–3] speed,[1,2,4] normal force,[1,4,5] apparent contact area,[1,5,6] roughness,[6,7] surface structure,[6,7] wettability,[7,8] icephobicity,[7,8] relative humidity (RH),[1] and thermal conductivity.[9] Considering the conditions inherent in ski applications, temperature, speed, normal force, apparent contact area, relative humidity, and thermal conductivity are difficult to be controlled. On the other hand, surface structure, roughness, wettability, and icephobicity are correlated factors.

A change in the surface morphology can be used to tune the surface response in terms of wettability and icephobicity. Surface modifications can be achieved using different methods, among which laser surface texturing (LST) is a promising and flexible method for introducing changes in the surface morphology at different dimension scales, ranging from millimeter

[a]Electronic mail: francesco.ripamonti@polimi.it

to submicrometer. Moreover, the LST process can be adapted for use in large-scale industrial production.

In the most common case, a laser beam is used to generate a micrometric surface pattern, thereby changing the surface morphology and roughness. The surface texture geometry, dimension, and periodicity all have a direct impact on the surface wettability.[10–12] Hydrophobicity, in particular, governs the repelling of water from the surface,[13] and thus, controlling the wettability of a solid surface can be used to predict its friction against ice.[7,8]

In actuality, another key feature characterizing a surface with low friction against ice or snow is icephobia. Icephobia concerns the ability of a surface to prevent icing of the water that condenses or flows over it as well as to ensure a low adhesion force in the eventuality that ice is formed. In turn, icephobicity is correlated with the water wettability and hence is affected by surface morphology and roughness.

Kietzig *et al.*[1] have shown that it is possible to turn a metal surface superhydrophobic by generating an ordered surface roughness by laser processing, leading to a lowering of the friction coefficient. The effect is more evident near the ice melting point, where the film of liquid water between the contacting surfaces becomes thicker. Concerning icephobicity, Susoff *et al.*[7] have observed that an increase in surface roughness leads to an incremental increase in the adhesion strength of ice on the surface. Bharathidasan *et al.*[8] have confirmed this result and further reported that hydrophobic materials exhibit an icephobic behavior more pronounced than superhydrophobic materials. Therefore, despite a strong correlation between the two behaviors, maximizing the contact angle (CA) does not necessarily correspond to an increased icephobicity, and the effect of surface texture should thus be assessed as a whole. The requirement of a low friction coefficient on ice has been investigated in application fields ranging from aerospace to naval,[14–16] but there is yet a lack of data concerning competitive winter sports.[17,18]

In this work, we discuss the effect of different surface textures on innovative metallic ski bases. In particular, stainless steel and an aluminum alloy were tested both in "untreated" and in "laser surface textured" conditions. Moreover, the morphology and water contact angles were assessed. Finally, the performance of these solutions was characterized using a custom-built snow tribometer, able to operate under controlled temperature and humidity conditions. The tangential force between the materials and the snow surface was measured, and a friction coefficient model was evaluated.

II. EXPERIMENTAL RESULTS

A. Materials

Two metallic materials were tested along with the more conventional ski material UHMWPE. Stainless steel (AISI 301, Lamina S.p.A., Milano, Italy) was selected for both its excellent mechanical characteristics and its good resistance to corrosion in an aqueous environment. The specimens were cold-rolled to a 0.5 mm-thickness. The commercial Al alloy Titanal® (AMAG Austria Metall AG, Ranshofen, Austria) was chosen, which is a low-density metal already employed in ski manufacturing, and the specimens used were 0.4 mm thick. The nominal compositions and mechanical properties of the two materials are reported in Tables I–III.

TABLE I. AISI 301 chemical composition (data from Lamina S.p.A.).

AISI 301	C%	Mn%	P%	S%	Si%	Cr%	Ni%	N%
	0.15	2.00	0.0045	0.030	0.75	16.00–18.00	6.00–8.00	0.10

TABLE II. Titanal chemical composition (data from AMAG_Austria Metal AG).

Titanal	Al%	Cu%	Mg%	Zn%	Zr%
	88.7	1.7	2.5	7	0.1

B. Surface treatment design and patterning

We note that the UHMWPE and pristine Titanal bases were prepared with an imprint, which is a typical procedure adopted by ski manufacturers, similar to a surface multidirectional scratch. Both bases were able to be applied with this procedure owing to the low hardness of both materials, wherein the process was compatible with material machinability.

In the LST process, we adopted dimples for our surface features, consisting of shallow blind holes with a low aspect ratio. The use of dimpled surfaces in the study of snow and ice friction has not been widely investigated; however, dimples have been shown to improve the tribological behavior of mechanical components. Applied to mechanical surfaces, they can reduce the friction coefficient by acting as lubricant reservoirs, they can contribute to load bearing by the generated hydrostatic pressure, and they can reduce third-body wear by entrapping the wear debris.[19,20] Moreover, dimples are symmetric features that allow us to avoid directionality in this initial attempt to determine the feasibility of surface textures to improve ski performance. Indeed, for a surface that undergoes friction along a single direction, the feature shape is a characteristic that can be easily optimized in further studies.[21]

Dimples can also have an impact on the surface wettability. The reduction in the contact area and the fact that high capillary forces are required to fill in the dimple cavities may increase the static contact angles.[22] However, compared to nanometric and hierarchical nano-/micrometric surface structures, the change in wettability is limited.[10]

A further important factor is the simplicity of the dimple geometry. Compared to more complex nanometric features, such as laser-induced periodic surface structures achieved

TABLE III. Mechanical properties relevant to ski bases for UHMWPE, AISI 301, and Titanal (data from Lamina S.p.A. and AMAG_Austria Metal AG).

Material	Brinell hardness	Tensile strength (MPa)	Yield stress (MPa)
UHMWPE	40	48	21
AISI 301	588	1802	1613
Titanal	207	630	580

with femtosecond-pulsed lasers, dimpling with nanosecond-pulsed lasers provides a higher productivity.

The dimple diameter (d) and depth (h) were controlled via the laser percussion microdrilling process, while the dimple spatial distribution was defined by the positioning of the laser beam by the scanner head. In this work, the dimples were realized with a fixed pitch (p) in both the horizontal and vertical directions. An industrial nanosecond fiber laser source (IPG Photonics YLP 1/100/50/50) was used to realize the texture. Beam handling was performed via a scanner head (TSH 8310, Sunny Technology, Beijing, China) equipped with an f-theta lens possessing a 100 mm focal length, thus obtaining a minimum beam spot diameter (d_0) of 39 μm. A point-by-point laser percussion drilling strategy produced dimples,[23] where the process parameters were chosen to obtain the desired pattern in terms of diameter and depth on the two different metals. The characteristics of the produced dimples are reported in Table IV. Figure 1 shows representative focus variation microscopy images of the laser-textured metallic surfaces, prepared according to the parameter values given in Table IV.

Water CAs were measured with a sessile drop system using 2 μl of distilled water.[24] The produced patterns induced an alteration of the water contact angle. Figure 2 shows the contact angle measurements of the metallic surfaces before (i.e., pristine) and after LST, where we observe that before texturing, both the materials are characterized by a hydrophilic behavior (CA $< 90°$) with average contact angles around 75°. The introduction of dimples led to an increase in the contact angle values, shifting the average values into the hydrophobic region (CA $> 90°$), with average values of about 110° for AISI 301 and 120° for Titanal. Such an increase can be interpreted in terms of entrapment of air within the dimples which sustains the water droplet above the metal surface.[22]

C. Evaluation of the friction coefficient against snow

1. Design of a custom-built snow tribometer

To characterize the tribological behavior of the samples, a snow tribometer was developed. To ensure that the snow was not melted, the tribometer was positioned in a climatic chamber (Model MKF-720, Binder GmbH, Tuttlingen, Germany), allowing for temperatures between +180 and −40 °C [Fig. 3(a)]. The temperature was monitored by a Pt100 sensor with a maximum fluctuation of ±0.5 °C with respect to the set-point. Ambient humidity was also controlled and monitored via a hygrometer (humidity ranging from 10% to 98% RH).

TABLE IV. Process parameters and average geometric properties of dimples produced on AISI 301 and Titanal.

Parameter	AISI 301	Titanal
Pump current (%)	100	100
Pulse repetition rate (kHz)	50	50
Modulation time, t_{mod} (μs)	70	70
Dimple diameter, D (μm)	35 ± 3	43 ± 1
Dimple depth, h (μm)	15 ± 3	38 ± 5

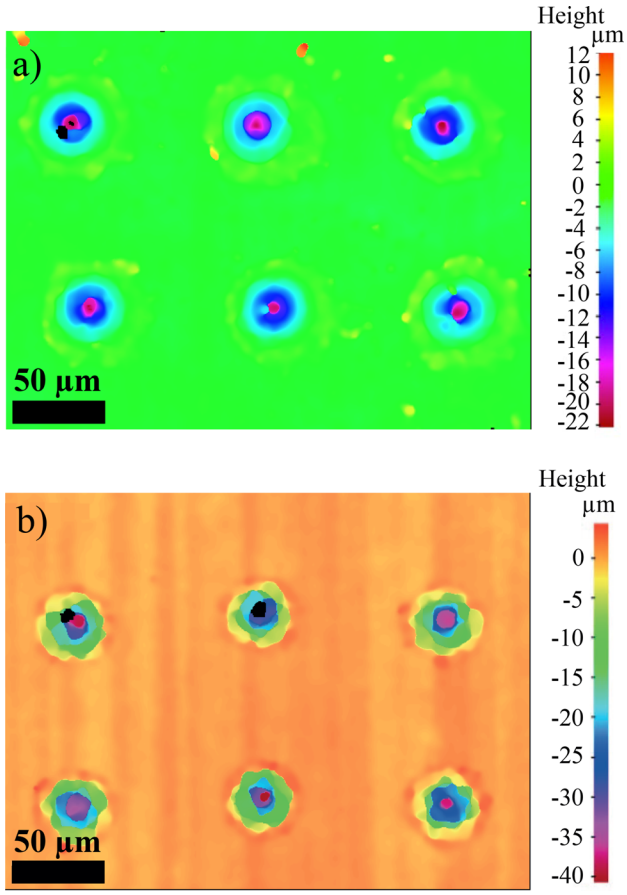

FIG. 1. (Color online) Focus variation microscopy images of the dimpled surfaces on (a) AISI 301 and (b) Titanal.

The tests discussed here were all conducted at −10 °C, with an RH of 50%.

The tribometer was based on a rotating snow bed and a stationary sample holder. Inside a circular plate of aluminum (400 mm in diameter and 100 mm in height), we placed a circular seat adapted to contain the snow. The plate was keyed via a shaft and a bushing to a 250 W electric motor, where the engine was then connected to the tribometer frame by means of an aluminum cylindrical support and two roller bearings.

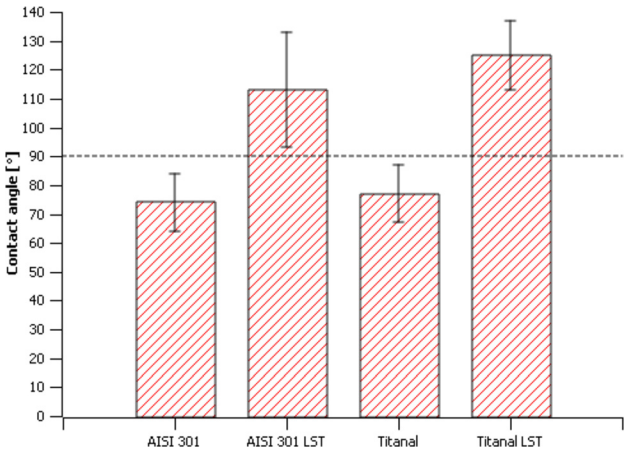

FIG. 2. (Color online) Comparison between contact angles of pristine and textured surfaces for AISI 301 and Titanal.

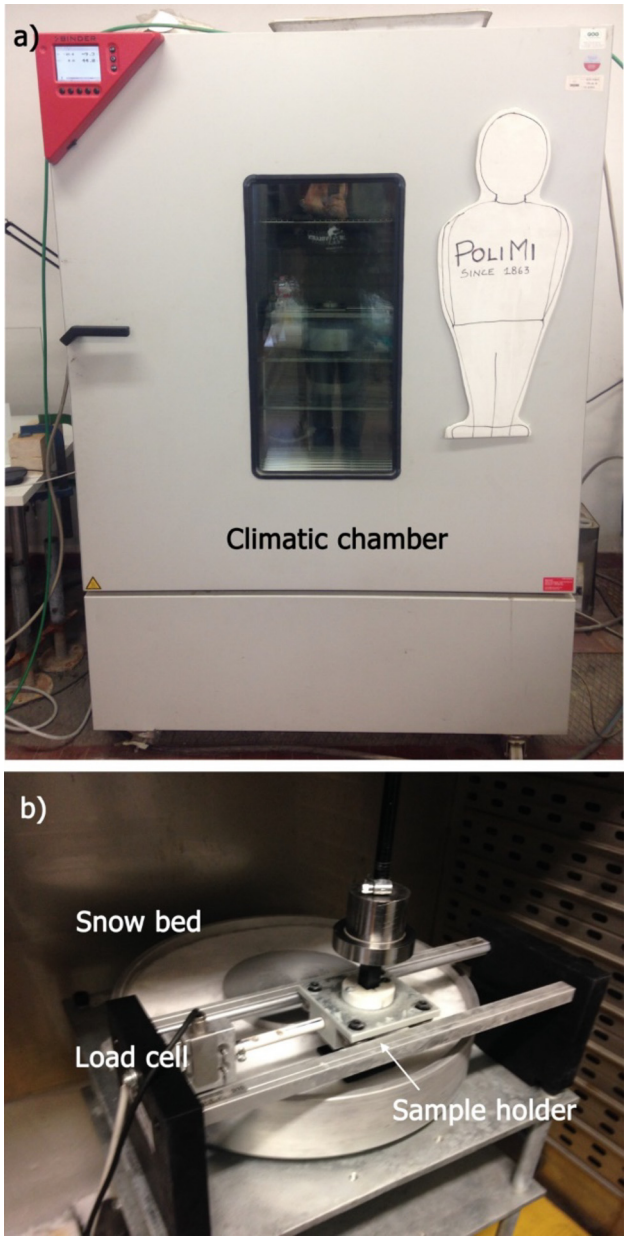

FIG. 3. (Color online) Photographs of the custom-built snow tribometer (a) positioned in a climatic chamber and (b) a close-up of the experimental setup.

These bearings were sized to have a minimum resistance opposing the force provided by the motor to rotate the plate.

On the top plate, two rectangular supports were mounted that held two rails on which a carriage bearing the sample holder ran. The sample holder was made of acrylonitrile butadiene styrene and shaped to match a ski tip. A 1.6 mm-deep pocket with the area dimensions of $50 \times 50\,\text{mm}^2$ was used to insert the ski bases to be tested, which were affixed to the pocket with double-sided tape. To measure the tangential force, the sample holder was connected to a load cell (Model CTCA1K5, AEP transducers, Modena, Italy) with a nominal load of 10 N and a nominal sensibility of 2 mV/V. The electric motor was connected to a controller to regulate the rotation speed.

Upon starting the electric motor, the rotation produced a tangential friction force between the snow bed and the test specimen, where the force was measured by the load cell connected to the sample holder. Figure 3(b) shows photographs of the experimental arrangement.

TABLE V. Tested base materials and their surface treatments.

Sample material	UHMWPE	AISI 301	Titanal
Treatment	Waxed	Pristine laser textured	Pristine laser textured
Sample thickness (mm)	1.6	0.5	0.4

2. Test conditions

Five different samples corresponding to various sample materials and surface treatments were prepared and tested, which are reported in Table V. Each sample was tested three times, resulting in a total number of 15 different tests.

A key point in tribological testing against snow is the management of temperature and snow conditions throughout the tests. It requires careful planning to test 15 samples as a function of different rotational speeds, while taking into account the possible changes in snow track conditions. A preliminary campaign of tests was conducted to determine the snow conditions most suited to guarantee the repeatability of the measurements. The snow bed must be carefully prepared by packing and partially icing the natural snow to closely approach the conditions of a slope prepared for a high-level competition (i.e., consisting of packed, icy snow). Under such conditions, it was possible to perform an acceptable number of reliable tests before holes were incidentally formed by the sample along the track. Indeed, whenever the track lost its flatness, the test had to be stopped and the track integrity restored.

Each test was performed with a stepped increase of the rotational speed from 100 to 1000 rpm, where the speeds used herein are specified in Table VI. At each rotational speed, a permanence stage of 40 s was set to establish steady track conditions and thus steady conditions in terms of the registered tangential force.

Figure 4 shows a representative example of the force measurement results. In these measurements, each specimen was tested by applying five consecutive runs, where the tribometer was stopped after each run. At the end of the fifth run, a new specimen was mounted and the temperature and the relative humidity of the climatic chamber were stabilized at the reference values. A random sequence was followed to test the 15 different samples.

III. FRICTION MODEL

A. Performance tests

To calculate the friction coefficient via tribometer tests, the rotational speed imposed by the electric motor and the tangential friction force measured by the load cell were

TABLE VI. Motor rotation speeds used for the snow tribometer tests.

Parameter	Value
Snow plate rotational speed (rpm)	100-200-300-400-500-600-800-1000

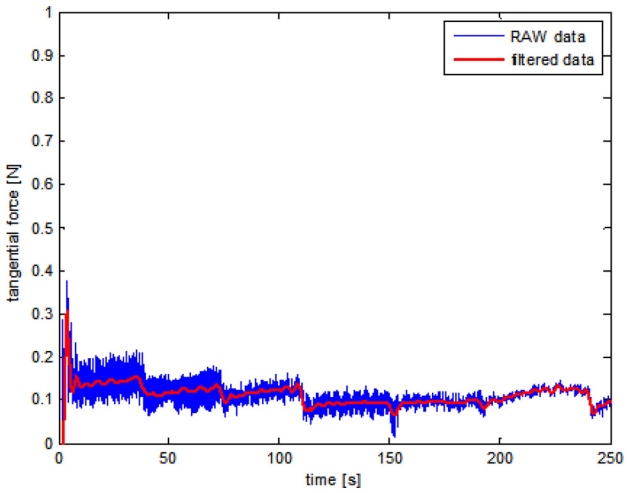

FIG. 4. (Color online) Representative tangential force results, where the stepped speed increase is evident.

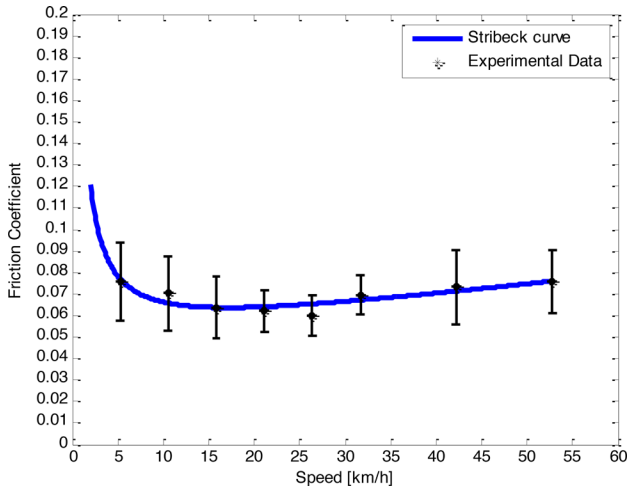

FIG. 5. (Color online) Assessment of the Stribeck curve for the UHMWPE sample.

collected. A simple model was used to analyze the data, which was based on the following equations:

$$\omega = \frac{2 \cdot \pi \cdot \text{rpm}}{60} \tag{1}$$

and

$$v = \omega \cdot d, \tag{2}$$

where rpm (rad/s) is the rotational speed of the electric motor, ω is the angular speed of the plate containing the snow (rad/s), v is the tangential speed of the sample (m/s), and d is the distance between the center of the plate and the center of the sample (140 mm). This information allows us to calculate the equivalent skier speed (km/h).

It is now possible to calculate the friction coefficient, considering that the normal force is given as

$$F_N = m \cdot g, \tag{3}$$

and the tangential force by

$$F_t = \mu \cdot F_N, \tag{4}$$

where the mass m is chosen to simulate the average pressure distribution of an average actual skier (kg), g is the gravitational acceleration (9.81 m/s^2), and the forces F_N and F_t are measured in N. The dimensionless friction coefficient μ is calculated as

$$\mu = \frac{F_t}{F_N}. \tag{5}$$

Taking a ski that is 1700 mm in length with an average width of 85 mm, the contact area of two skis is 289 000 mm^2. Knowing that the area of the samples is 2500 mm^2 and considering a skier mass of about 70 kg, it is possible to calculate the equivalent mass value using

$$m = \frac{70 \times 2500}{289\,000} = 0.605\,\text{kg}. \tag{6}$$

For each tested condition (see Table V) and for each speed step, different values of the friction coefficient were found. These values were analyzed, and their normal distribution was calculated using the least-squares method. These results were used to determine the best curve, fitting the experimental values with the Stribeck model[25]

$$\mu_{\text{stribeck}} = \mu_0 + \mu_1 v + \frac{\mu_2}{v}, \tag{7}$$

where μ_{stribeck} is the friction coefficient; μ_0, μ_1 and μ_2 are constants, and v is the varying test speed.

B. Results and discussion

Figure 5 shows an example of curve fitting of the experimental data obtained for a UHMWPE ski base. The procedure was repeated for all test conditions, which include varying the materials, preparation, and rotational speed, and the results are summarized in Fig. 6.

Table VII shows the coefficients used to calculate the friction coefficient according to the Stribeck model [Eq. (7)] for the different tested samples.

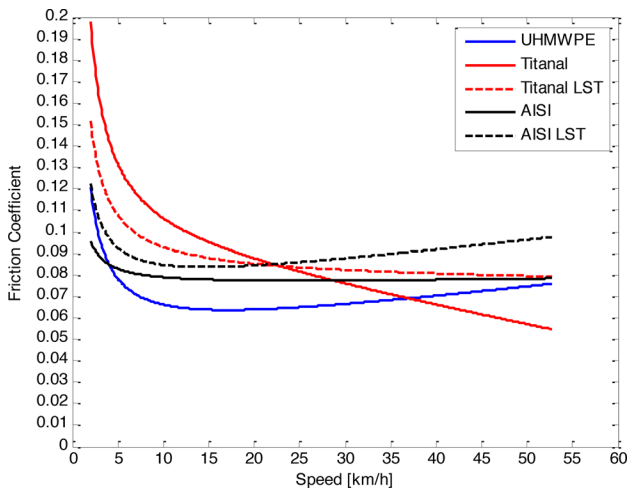

FIG. 6. (Color online) Comparison between gliding performances of different samples.

TABLE VII. Coefficients of the Stribeck friction model for each sample.

Sample	μ_0	μ_1	μ_2
UHMWPE	0.046	5.06×10^{-4}	0.147
AISI 301	0.074	6.97×10^{-5}	0.043
AISI 301 LST	0.069	5.01×10^{-4}	0.105
Titanal	0.093	-8.09×10^{-4}	0.212
Titanal LST	0.079	-4.32×10^{-5}	0.146

The UHMWPE exhibits the lowest friction coefficient values, thus corresponding to the best performance of the ski base at all speeds. This result is not particularly surprising considering that all the tested UHMWPE samples were waxed using the state of the art, while no wax-equivalent treatments were applied to the metallic samples. This choice was deliberately made to compare metal base performances with the best bases presently available.

The laser-treated AISI 301 presents a trend similar to UHMWPE, although with slightly higher μ_0 and μ_1 values (about +25%). The adopted, nonoptimized LST affects the metal ski surface at the micrometer scale and results in an increase in the apparent contact area between the ski and the snow. This produces an increase in the number of surface asperities and thus in an increase in the friction coefficient uncompensated by the concomitant hydrophobicity increase induced by the LST (see Fig. 2).

Pristine AISI 301 and laser-treated Titanal display a trend almost independent of speed. Such a behavior is not surprising since it has been previously reported for UHMWPE over a wide range of temperatures and speed values,[2] including those explored herein. However, at speeds higher than 55 km/h, it is likely that an inversion with respect to UHMWPE can occur.

Pristine and LST Titanal present a trend that differs from all the other typologies, exhibiting very high friction coefficient values at low speeds and their lowest values at the highest speeds, which signifies a negative μ_1 coefficient (see Table VII). This phenomenon is owing to the surface imprinting rather than LST machining. As a result, the minimum position, typical of the Stribeck model of friction,[25] shifts beyond the upper speed explored in the present study (50–55 km/h).

We recall that the UHMWPE and pristine Titanal are the only solutions on which an imprint was applied. The procedure produces an increase in the detachment friction coefficient, but it also reduces the friction at higher speeds. This is also the reason for the observed crossover point for the Titanal pristine and LST at a midlow speed (22 km/h). Similarly, the break-even point between UHMWPE and Titanal pristine occurs at the midhigh speeds (35–40 km/h), while at 50 km/h the improvement is about −30%.

IV. CONCLUSIONS

This work uses different materials in the construction of a ski base, particularly focusing on metallic materials that exhibit a good gliding behavior on compact, icy, dry snow. From the laboratory tests, it is possible to deduce how the two metallic materials of AISI 301 stainless steel and aluminum alloy (Titanal) behaved similar to UHMWPE when gliding on this sort of snow. Both metals exhibit slightly worse gliding at low speeds but possess low friction coefficients at high speeds.

The micrometer-scale dimple texture produced by laser treatment does not significantly improve the performance of both types of metals in contact with snow, despite the presence of a hydrophobic behavior on the machined materials. On Titanal, the LST improves the friction coefficient at low speeds but degrades it at high speeds. On AISI 301, the friction coefficient values are similar in LST-treated and pristine samples without any meaningful increase in the performances. A modeling study to optimize the feature size, shape, and spacing is planned for ongoing work.

ACKNOWLEDGMENT

The authors would like to acknowledge Blossom Skis (Prata Camportaccio, Italy) for technical and financial contributions to this research.

[1]A. M. Kietzig, S. G. Hatzikiriakos, and P. Englezos, J. Appl. Phys. **107**, 081101 (2010).
[2]L. Makkonen and M. Tikanmäki, Cold Reg. Sci. Technol. **76–77**, 24 (2012).
[3]L. Baurle, D. Szabò, M. Fauve, H. Rhyner, and N. D. Spencer, Tribol. Lett. **24**, 77 (2006).
[4]R. Böttcher, M. Seidelmann, and M. Scherge, Cold Reg. Sci. Technol. **141**, 171 (2017).
[5]S. Rohm, M. Hasler, C. Knoflach, J. van Putten, S. H. Unterberger, K. Schindelwig, and W. Nachbauer, Tribol. Lett. **59**, 27 (2015).
[6]A. M. Kietzig, S. G. Hatzikiriakos, and P. Englezos, J. Appl. Phys. **106**, 024303 (2009).
[7]M. Susoff, K. Siegmann, C. Pfaffenroth, and M. Hirayama, Appl. Surf. Sci. **282**, 870 (2013).
[8]T. Bharathidasan, S. V. Kumar, M. S. Bobji, R. P. S. Chakradhar, and B. J. Basu, Appl. Surf. Sci. **314**, 241 (2014).
[9]A. M. Kietzig, S. G. Hatzikiriakos, and P. Englezos, J. Galciol. **56**, 473 (2010).
[10]A. M. Kietzig, S. G. Hatzikiriakos, and P. Englezos, Langmuir. **25**, 4821 (2009).
[11]P. Bizi-Bandoki, S. Benayoun, S. Valette, B. Beaugiraud, and E. Audouard, Appl. Surf. Sci. **257**, 5213 (2011).
[12]A. G. Demir, V. Furlan, N. Lecis, and B. Previtali, Biointerphases **9**, 029009 (2014).
[13]A. B. D. Cassie and S. Baxter, Trans. Faraday Soc. **40**, 546 (1944).
[14]L. O. Andersson, C. G. Golander, and S. Persson, J. Adhes. Sci. Technol. **8**, 117 (1994).
[15]S. Frankenstein and A.-M. Tuthill, J. Cold. Reg. Eng. **16**, 83 (2002).
[16]K. Golovin, S.-P.-R. Kobaku, D. H. Lee, E. T. DiLoreto, J. M. Mabry, and A. Tuteja, Sci. Adv. **2**, 1501496 (2016).
[17]S. C. Colbeck, J. Sports Sci. **12**, 285 (1994).
[18]G. De Koning, G. J. De Groot, and J. V. I. Schenau, J. Biomech. **25**, 565 (1992).
[19]I. Etsion, J. Tribol. **127**, 248 (2005).
[20]A. Erdemir, Tribol. Int. **38**, 249 (2005).
[21]H. Yu, X. Wang, and F. Zhou, Tribol. Lett. **37**, 123 (2010).
[22]P. Maressa, L. Anodio, A. Bernasconi, A. G. Demir, and B. Previtali, J. Adhes. **91**, 518 (2015).
[23]A. G. Demir, B. Previtali, and N. Lecis, Opt. Laser Technol. **54**, 53 (2013).
[24]ASTM D7334–08, *Standard Practice for Surface Wettability of Coatings, Substrates and Pigments by Advancing Contact Angle Measurement* (2013).
[25]H. Czichos and K. H. Habig, *Tribologie-Handbuch (Tribology Handbook)*, 2nd ed. (Vieweg Verlag, Wiesbaden, 2003).